ELSEVIER

Palaeogeography, Palaeoclimatology, Palaeoecology 141 (1998) 233–251

PALAEO

Late Quaternary precessional cycles of terrigenous sediment input off the Norte Chico, Chile (27.5°S) and palaeoclimatic implications

Frank Lamy *, Dierk Hebbeln, Gerold Wefer

Fachbereich Geowissenschaften, Universität Bremen, Postfach 33 04 40, D-28334 Bremen, Germany

Received 4 November 1997; accepted 23 January 1998

Abstract

The palaeoclimatic conditions during the Last Glacial Maximum (LGM) of southern South America and especially latitudinal shifts of the southern westerly wind belt are still discussed controversially. Longer palaeoclimatic records covering the Late Quaternary are rare. A particularly sensitive area to Late Quaternary climatic changes is the Norte Chico, northern Chile, because of its extreme climatic gradients. Small shifts of the present climatic zonation could cause significant variations of the terrestrial sedimentary environment which would be recorded in marine terrigenous sediments. To unveil the history of shifting climatic zones in northern Chile, we present a sedimentological study of a marine sediment core (GeoB 3375-1) from the continental slope off the Norte Chico (27.5°S). Sedimentological investigations include bulk- and silt grain-size determinations by sieving, Atterberg separation, and detailed SediGraph analyses. Additionally, clay mineralogical parameters were obtained by X-ray diffraction methods. The ^{14}C-dated core, covering the time span from approximately 10,000 to 120,000 cal. yr B.P., consists of hemipelagic sediments. Terrigenous sedimentological parameters reveal a strong cyclicity, which is interpreted in terms of variations of sediment provenance, modifications of the terrestrial weathering regimes, and modes of sediment input to the ocean. These interpretations imply cyclic variations between comparatively arid climates and more humid conditions with seasonal precipitation for northern Chile (27.5°S) through the Late Quaternary. The cyclicity of the terrigenous sediment parameters is strongly dominated by precessional cycles. For the palaeoclimatic signal, this means that more humid conditions coincide with maxima of the precession index, as e.g. during the LGM. Higher seasonal precipitation for this part of Chile is most likely derived from frontal winter rain of the Southern Westerlies. Thus, the data presented here favour not only an equatorward shift of this atmospheric circulation system during the LGM, but also precession-controlled latitudinal movements throughout the Late Quaternary. Precessional forcing of latitudinal movements of the westerly atmospheric circulation system may be conceivable through teleconnections to the Northern Hemisphere monsoonal system in the Atlantic Ocean region.

Keywords: Chile; clastic sediments; palaeoclimatology; Quaternary; cycles; precession

* Corresponding author. Fax: 49-421 218 3114; E-mail: frankl@allgeo.uni-bremen.de

0031-0182/98/$19.00
PII S0031-0182(98)00052-2

1. Introduction

Palaeoclimatic records from southern South America and the adjacent Southeast Pacific are rare. Existing reconstructions include exclusively continental records which are primarily based on palynological data from central to southern Chile and Argentina (e.g. Heusser, 1990; Markgraf et al., 1992; Villagrán, 1993). Additionally, glaciological (review in Clapperton, 1993), limnological (e.g. Grosjean et al., 1995) as well as geomorphological and pedological studies (e.g. Veit, 1996) have been carried out in order to reconstruct the palaeoclimatic evolution, basically since the Last Glacial Maximum (LGM). Longer palaeoclimatic time-series (e.g. Heusser, 1984; Clapperton et al., 1995; Lowell et al., 1995) are rare and the age control of continental records is often problematic.

During the LGM, latitudinal shifts of the South American atmospheric circulation systems, especially of the Southern Westerlies, were proposed. However, it is still being discussed whether the latitudinal shift was equatorward (e.g. Heusser, 1989) or poleward (Markgraf, 1989). More recently, modelling studies for the LGM palaeoclimate of Patagonia (Hulton et al., 1994) and glacier fluctuations in southernmost Chile (Clapperton et al., 1995) support a moderate northward shift of the Westerlies.

In this paper we present a marine palaeoclimatic data set, comprising the last 120,000 years, as recorded in terrigenous sediments on the continental slope off the Norte Chico, northern Chile. This region is particularly suitable to study Late Quaternary climatic changes, due to the extreme modern climatic gradients at the southern boundary of the Atacama desert (Miller, 1976). Thus, small shifts of the present atmospheric circulation systems could cause significant climatic changes and modifications of the terrestrial sedimentary environment, which may alter the terrigenous sediment input to the ocean and, thus, to the core position.

Due to robust and high resolution age-control, our palaeoclimatic record provides the opportunity to investigate climatic changes of southern South America throughout the Late Quaternary. Particularly latitudinal movements of the Southern Westerlies are recorded and insight into cyclicity and forcing of these movements is given.

2. Study area

The analysed sediment core GeoB 3375-1 was taken from the continental slope off the Norte Chico, northern Chile at approximately 27.5°S (Fig. 1A). This area is characterized by an extremely narrow shelf, only 10 to 15 km wide on average, and a deep, only partially sediment-filled trench reaching maximal water depths of 7000 m (Scholl et al., 1970). The continental slope is generally steep, with maximum inclinations of 10° to 15° in the lower part. The middle part is less inclined and often comprises structural terraces or troughs which form sediment traps (Scholl et al., 1970). At 27.5°S two terrace-shaped sectors occur, one at water depths of 1900 to 2100 m and the second at 2400 to 2600 m (shipboard Parasound data). Core GeoB 3375-1 was taken near the landward edge of the first terrace.

The oceanographic setting is characterized by two equatorward flowing surface currents: the Humboldt Current (HC, Fig. 1A) and the Chile Coastal Current (CCC, Fig. 1A). The HC, which originates from the Antarctic Circumpolar Current, transports Subantarctic Surface Water northward and is located 100–300 km offshore (Strub et al., 1998). The poleward flowing Peru–Chile Countercurrent (PCC, Fig. 1A) separates the HC and CCC. The CCC is more variable, consists of a narrow band of comparatively low-salinity water from the South Chilean fjord region, and is part of the coastal upwelling system (Strub et al., 1998). The most important subsurface current is the Gunther Undercurrent (GUC, Fig. 1A), transporting Equatorial Subsurface Water poleward, and is located primarily over the continental slope and outer shelf (Strub et al., 1998). The GUC reaches maximal velocities of up to 25 cm/s between 150 and 300 m water depth (Johnson et al., 1980; Shaffer et al., 1995). Antarctic Intermediate Water flows equatorward below 400 to 600 m water depth. It is underlain by sluggish poleward flowing Pacific Deep Water. The deepest parts of the Peru–Chile trench are filled with equatorward flowing Antarctic Bottom Water (Ingle et al., 1980).

The main morphological and geological features of the continental hinterland are the Coastal Range and the Andes (Fig. 1B). The Coastal Range rises rather abruptly from the coast to elevations of 2000 to 2500 m. It consists primarily of Mesozoic in-

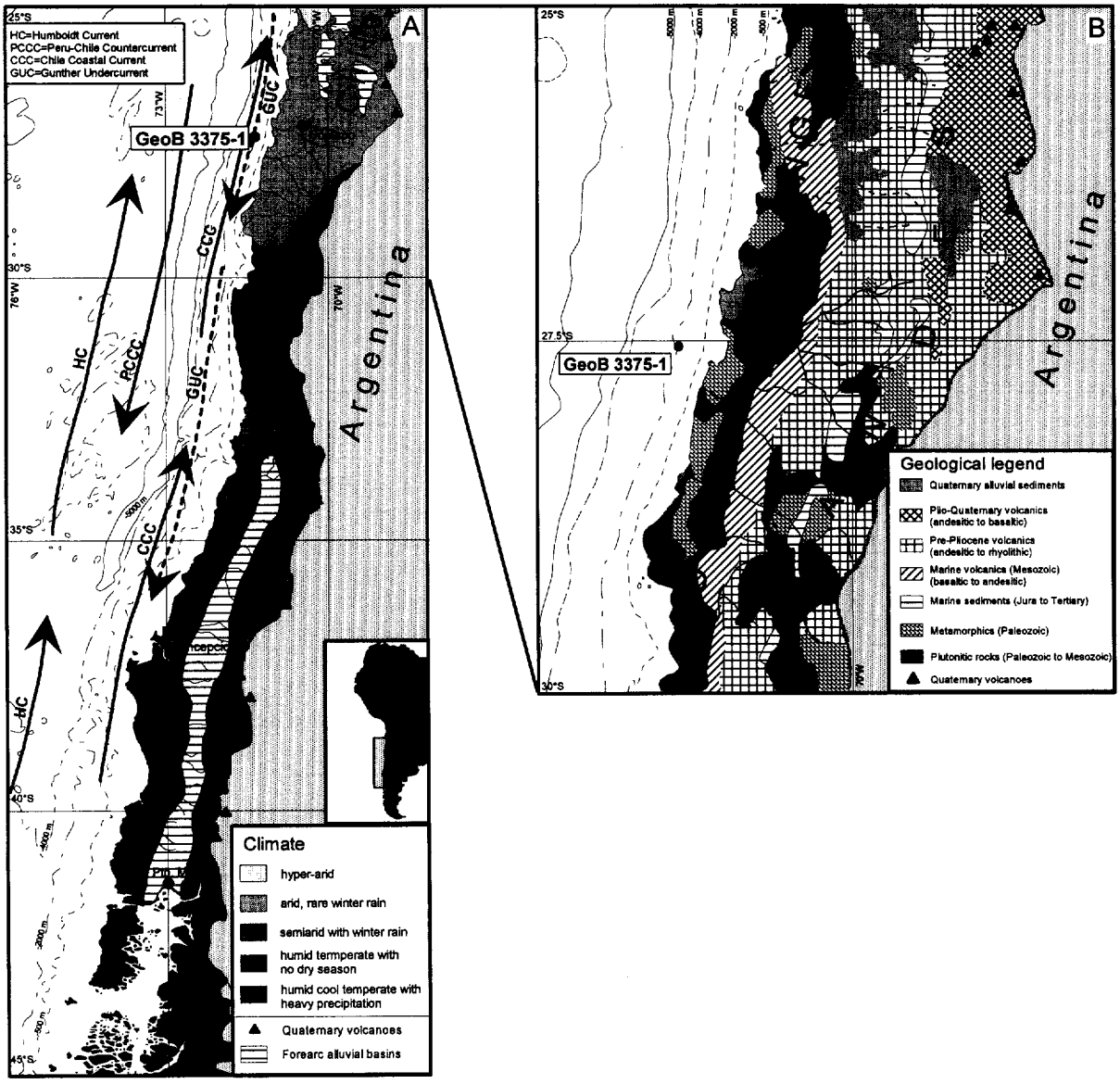

Fig. 1. (A) Map of the study area with location of core GeoB 3375-1 and principal oceanographic features (after Strub et al., 1998). Distribution of Quaternary volcanism and forearc alluvial basins (after Thornburg and Kulm, 1987b), continental hydrology and climatic zonation (after Heusser, 1984). (B) Geological map of Chile between 25°S and 30°S (after Zeil, 1986 and Thornburg and Kulm, 1987b). Dashed lines in the northern part indicate recent dry valleys.

termediate calc-alkaline plutonitic rocks and subordinately of metamorphics and basaltic to andesitic volcanics (Fig. 1B; Zeil, 1986; Thornburg and Kulm, 1987b). A major tectonic discontinuity divides the Andes in two segments (Fig. 1B). North of 27.5°S products of the Plio–Quaternary volcanism, including andesitic rocks and tephra overlying pre-Pliocene rhyolitic to andesitic ignimbrites, dominate the geology of the Andes (Zeil, 1986). In this area a longitudinal depression zone, marked by alluvial forearc basins which trap most of the sedimentary debris originating from the Andes, separates the Coastal

Range from the Andes (Zeil, 1986). South of 27.5°S Plio–Quaternary volcanism as well as alluvial fore-arc basins are absent, possibly due to a low-angle dipping subduction zone in this region (Jordan et al., 1983). The geological features of this southern Andean segment are characterized by pre-Pliocene volcanics which are similar to those of the northern segment, outcrops of Mesozoic plutonites and metamorphic basement, as well as sedimentary rocks (Zeil, 1986).

The modern climate of the region adjacent to the core position (Fig. 1A) is hyper-arid with precipitation values of <50 mm/a north of 27°S. Here begins the Atacama desert as part of the South American arid diagonal zone (Garleff et al., 1991). To the south annual precipitation increases slightly due to occasional passages of frontal systems of the Southern Westerlies (Miller, 1976), and episodic precipitation events occurring in this area in El Niño years (Veit, 1992). Only south of 31°S does the amount of winter rain increase significantly and a semiarid–mediterranean type climate is developed (Miller, 1976).

Transversal river valleys in the Coastal Range are nearly absent north of 27°S. The continental hydrology of this area is characterized by dry valleys with only sporadic water runoff (Abele, 1989). Further south perennial rivers originating in the Andean Cordillera generally cut through the Coastal Range (Weischet, 1970) but fluviatile discharge values are very low (Milliman et al., 1995). Even the Copiapo, a major river reaching the ocean close to our core location, presently does not supply significant discharges (0.07 km^3/a; Milliman et al., 1995). Due to these climatic and hydrologic conditions the modern sediment input to the continental slope in the area of 27°S can be attributed primarily to aeolian processes and/or episodic rapid sediment input after continental floodings in relation to El Niño events (Lamy et al., submitted).

3. Material and methods

Gravity core GeoB 3375-1 (27°28′S; 71°15′W; water depth 1947 m; core length 489 cm) was recovered during the CHIPAL-Expedition of RV *Sonne* (SO-102) at the continental margin of Chile (Hebbeln et al., 1995). The sediment core was sampled in steps of 5 cm using 10-ml syringes. Three sample series were taken. The first was designated for grain-size and clay mineral determinations and the second for oxygen isotope measurements. The third series was used for total organic carbon and carbonate measurements.

3.1. Grain-size measurements

In a first step the sediment was treated with 3.5% hydrogen peroxide to remove organic matter and disaggregation and with 10% acetic acid in order to solve carbonate. Due to low concentrations of opal and volcanic glass, no removal of amorphous SiO_2 was applied. Estimates of the amorphous SiO_2 content were deduced from X-ray powder diffraction (XRD) measurements and smear slide data.

The separation of the sand fraction (>63 μm) was achieved by wet-sieving, while the silt (2–63 μm) and clay fractions (<2 μm) were split by Stokes' law settling using Atterberg tubes (Müller, 1967). In order to separate the latter two size fractions almost completely, a 9–12 times repetition of the settling procedure was necessary. Coagulation of clay size particles was avoided by using a 0.1% sodium polyphoshate solution.

A detailed grain-size analysis of the silt fraction was performed by measurements with a Micromeritics SediGraph 5100. The SediGraph also detects remaining sand and clay particles in the silt fraction, which have not been removed by Atterberg- and sieving-methods. The SediGraph analysis provides a high resolution grain-size distribution in steps of 0.1 phi and is based on the X-ray scanning of a settling suspension assuming again Stokes' law settling. Detailed descriptions of the operating principles of this method can be found in Stein (1985), Jones et al. (1988), and Syvitszki (1991). Statistic grain-size parameters were calculated from the SediGraph data by formulas of Folk and Ward (1957).

Additional silt grain-size distributions of the carbonate fraction were calculated as proposed by McCave et al. (1995). The difference between the size distribution of the carbonate-free sediment and the size distribution of the bulk sediment, which was determined on a subsample, is interpreted as reflecting the size distribution of the carbonate silt fraction.

3.2. Clay mineralogy

The clay fraction was analysed for the four main clay mineral groups smectite, illite, kaolinite and chlorite following standard procedures described in detail by Petschick et al. (1996). The method is based on XRD measurements of oriented mounts of the Mg-saturated clay fraction. For our samples a Philips PW 1820 diffractometer with CoKα radiation (40 kV, 40 mA) was used and three XRD scans were run: firstly on the air-dry state (between 2° and 40° 2θ and a step size of 0.02°), secondly after ethylene glycol solvation (2°–40° 2θ; 0.02° step size) and finally a slow scan between 28° and 30.5° 2θ with steps of 0.005° 2θ was obtained on the glycolated mounts in order to distinguish the 3.54/3.58 Å kaolinite/chlorite double peak.

The diffractograms were evaluated with the 'MacDiff' software (Petschick, unpublished). Semi-quantitative clay mineral analysis was performed by weighting integrated peak areas of the main basal reflections in the glycolated state using smectite (17 Å), illite (10 Å) and kaolinite/chlorite (7 Å). Relative proportions of kaolinite and chlorite were determined by the evaluation of the slow scans (Petschick et al., 1996). Using the empirically estimated weighting factors of Biscaye (1965), relative percentages of the four clay mineral groups were obtained. Due to the dominance of chlorite, the calculation of kaolinite percentages, based on the evaluation of the slow scan, probably contains a significant error. Thus, especially for spectral analyses, the relative percentages of chlorite + kaolinite were used.

The crystallinity of illite and smectite was measured as the half height width (HHW) of the 10 Å illite peak and as the integral breadth (IB) of the glycolated 17 Å smectite peak, respectively. The IB represents the breadth ($\Delta°2\theta$) of an rectangle of the same area and height as the peak.

3.3. Carbonate determinations

Carbonate contents of the sediment were determined with an elemental analyser (Hereaus CHN-O-Rapid). Total carbon (TC) contents were measured on untreated samples and organic carbon (TOC) contents on HCl-treated samples. Carbonate contents were calculated according to the formula $CaCO_3 = (TC - TOC) \times 8.333$.

3.4. Stable oxygen isotope analyses

A Finnigan MAT 251 mass spectrometer with an automated carbonate preparation device was used to measure the stable oxygen isotope composition ($\delta^{18}O$) of the planktic foraminifera *Neogloboquadrina pachyderma* (sin.). Twenty individual shells (>212 μm) were picked for each measurement. The isotopic composition of the carbonate sample was measured on the CO_2 gas evolved by treatment with phosphoric acid at a constant temperature of 75°C. The ratio of $^{18}O/^{16}O$ is given in ‰ relative to the PDB standard. A working standard (Burgbrohl CO_2 gas) was used for measurement of the isotopic ratios of the samples NBS 18, 19, and 20 of the National Bureau of Standards. Analytical standard deviation is about ±0.07‰ PDB (Isotope Lab Bremen University).

3.5. ^{14}C-dates

Accelerator mass spectrometry (AMS) datings were carried out at the Leibniz Laboratory for Age Determinations and Isotope Research at the University of Kiel (Nadeau et al., 1997) using 10 mg carbonate (only shells of *N. pachyderma*). All ages are corrected for ^{13}C and for a reservoir age of 400 years (Bard, 1988). The ^{14}C-ages were converted to calendar years after the method of Bard et al. (1993).

3.6. Stratigraphy

The age model for core GeoB 3375-1 is based on three ^{14}C AMS dates (Table 1) in the upper

Table 1
Age control points of core GeoB 3375-1

Core depth (cm)	^{14}C AMS age (yr B.P.)	+ Err.	− Err.	Calendar age (yr B.P.)
13	9,760	100	100	11,262 [a]
118	20,060	330	320	23,722 [a]
183	34,460	2120	168	39,146 [a]
293	–	–	–	65,000 [b]
403	–	–	–	95,000 [c]
478	–	–	–	116,000 [c]

[a] Ages converted to calendar years following the method of Bard et al. (1993).
[b] Stage 4.2. of SPECMAP $\delta^{18}O$ stack (Imbrie et al., 1984).
[c] Maxima of the precession index (Berger and Loutre, 1991).

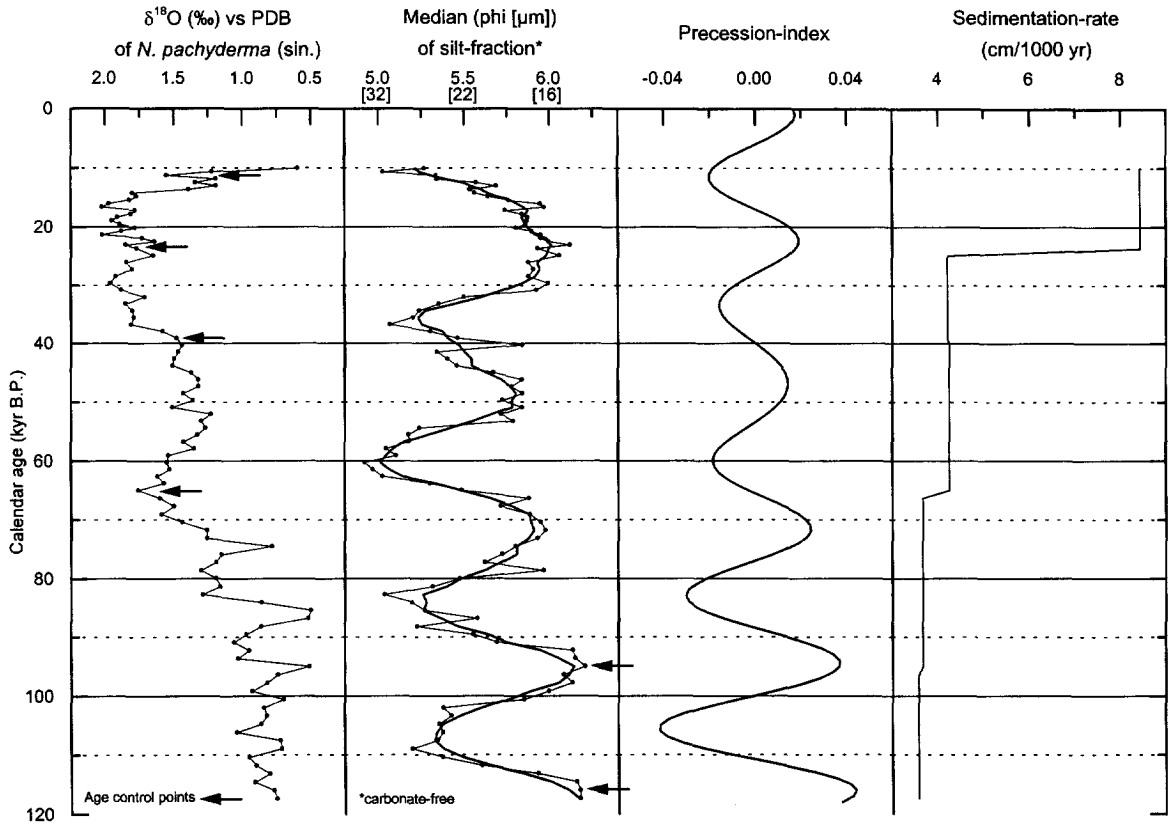

Fig. 2. Age model for sediment core GeoB 3375-1. Age control points (indicated by arrows, see Table 1) include three ^{14}C AMS dates and a graphical correlation point of the $\delta^{18}O$ record of *N. pachyderma* (sin.) with the SPECMAP $\delta^{18}O$ stack (Imbrie et al., 1984). Further downcore two more control points were obtained by correlation of the median of the silt fraction (thick line represents smoothed record performed by three point moving averaging) with the precession index (after Berger and Loutre, 1991). Resulting sedimentation rates are plotted to the right.

half of the core and a graphical correlation of the $\delta^{18}O$ isotope record of *N. pachyderma* (sin.) with the SPECMAP $\delta^{18}O$ stack (Imbrie et al., 1984). The age model resulting from these four age control points (Table 1) revealed that cyclic variations of grain-size parameters, best documented in the median of the silt fraction, strongly correlate to Earth's orbital precession (Fig. 2). For this reason, in the lower part of the core, we correlated grain-size minima of the median record to maxima of the precession index (Berger and Loutre, 1991, see Table 1, Fig. 2). Between age control points a linear interpolation was applied. On this basis, the core is estimated to cover the time span from approximately 10,000 cal. yr B.P. to 120,000 cal. yr B.P. corresponding to the marine isotope stages 1 to 5. The average sedimentation rate is 5 cm/1000 yr with above average values found during the isotope stage 2 interval (Fig. 2).

3.7. Spectral analyses

Time-series analyses were carried out with the SPECTRUM software package (Schulz, 1994). In contrast to widely used spectral analysis methods based on Blackman and Tukey calculation procedures (Blackman and Tukey, 1958), the SPECTRUM software does not require equidistant time-series. Thus, time-interpolation of the geological data was not applied.

4. Results

4.1. Grain-size data

The sediments of core GeoB 3375-1 can be classified as sandy clayey silts to clayey silts. Bulk grain-size parameters of the carbonate-free sediment reveal cyclic variations which correlate to Earth's orbital precession (Fig. 3A). The bulk sediment is generally coarser grained in core intervals related to precession minima and finer grained in intervals correlated to precession maxima. The amplitude of the cycles is approximately 10 to 15 wt% for sand- and clay-content records. Silt contents do not display a precessional cyclicity in the upper part of the core but further downcore cycles with amplitudes of approx. 10 wt% occur.

Silt grain-size data reveal precessional cycles throughout the core (Fig. 4). The silt fraction is coarser grained, better sorted, more positively skewed and strongly peaked (leptokurtic) in core intervals which correspond to precession minima. The reverse results occur for the precession maxima. For the extrema of each cycle contrasting silt grain-size distributions can be distinguished (Fig. 4). For the precession minima, grain-size distributions are unimodal, very positively skewed, better sorted, leptokurtic and reveal median values around 5 phi (32 μm). For the precession maxima, the distributions are also predominately unimodal, but nearly

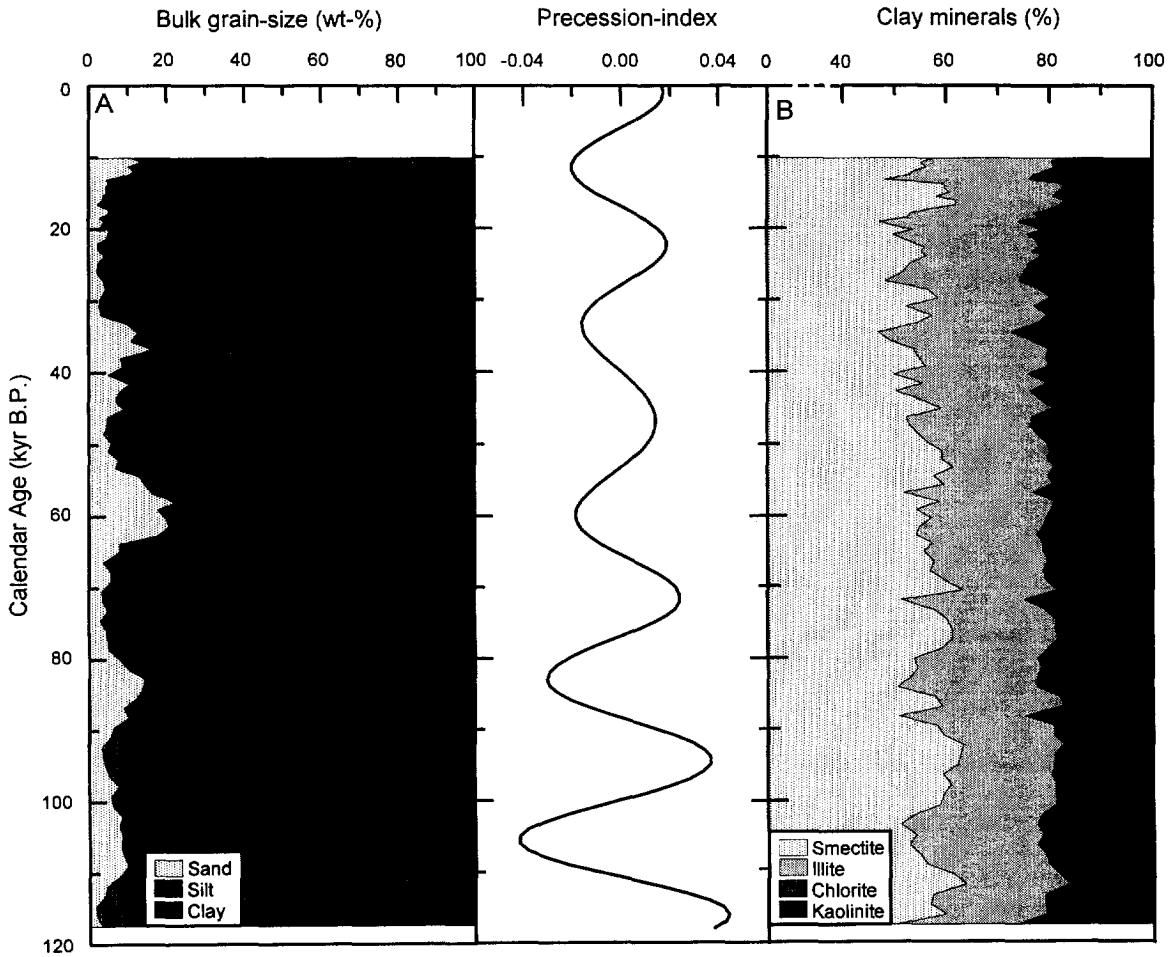

Fig. 3. (A) Bulk grain-size data, as represented by the relative percentages of sand, silt and clay (<2 μm). (B) Relative contents of the four clay mineral groups smectite, illite, chlorite and kaolinite. The precession index is plotted in the middle part of the figure.

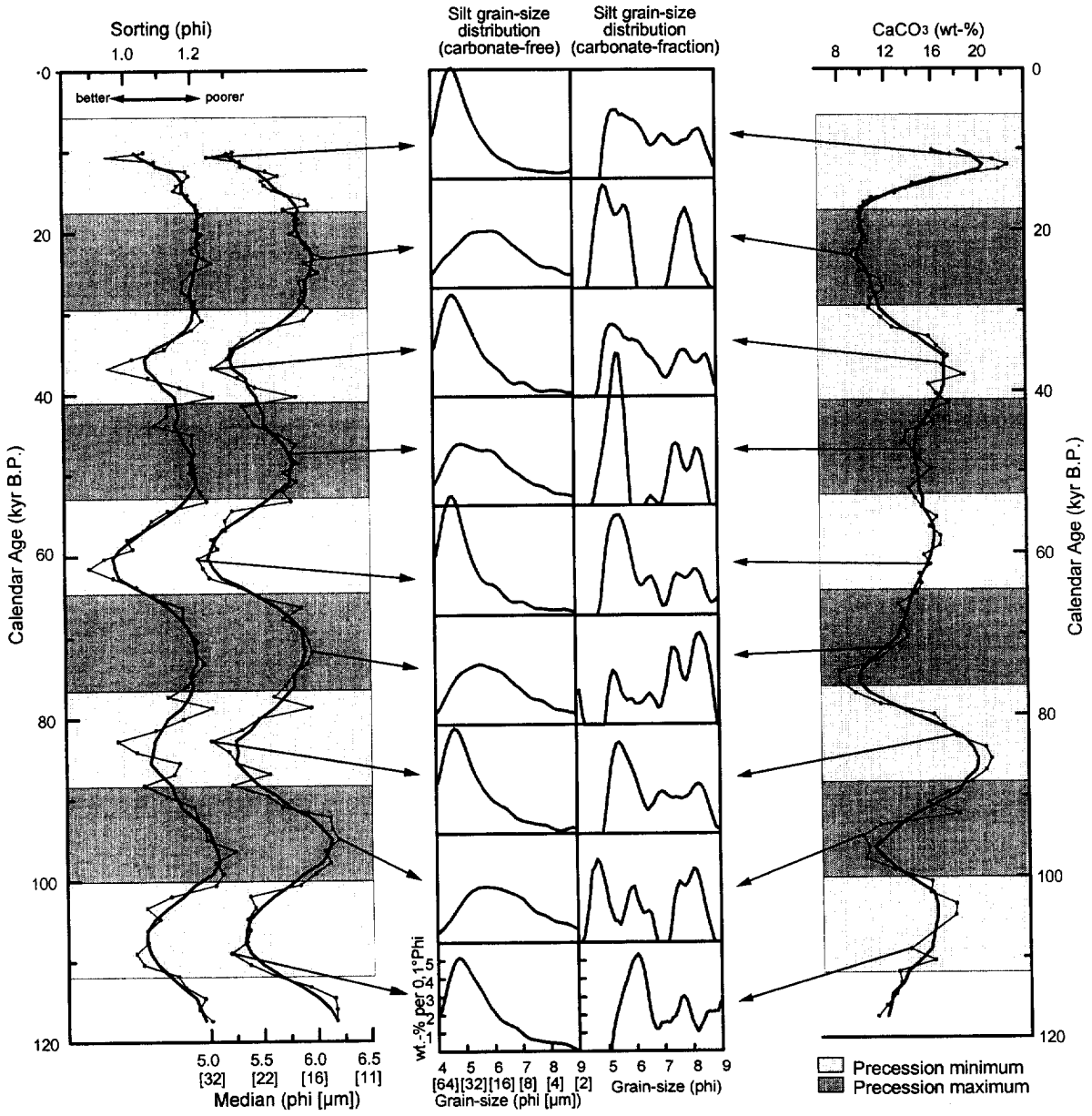

Fig. 4. Silt grain-size data. Sorting and median show cyclic variations. High resolution silt grain-size distributions are plotted for the extremes of each cycle for the carbonate-free fraction (left) and carbonate fraction (right). Additionally, the carbonate content record is shown on the right side. Thin lines with data points represent the original data set, thick lines are smoothed curves (except for silt grain-size distributions). The lines were smoothed by using a three point moving average. Core intervals related to precession minima are marked in light grey and those relating to precessional maxima in dark grey.

symmetrical, poorer sorted, poorly peaked (meso- to platykurtic) and exhibit medians of around 6 phi (16 µm).

4.2. Clay mineralogy

Clay mineral assemblages (Fig. 3B) are dominated by smectite (approx. 45 to 65%) and illite

(approx. 18 to 28%). Chlorite contents range from approximately 12 to 22%, kaolinite only occurs in minor amounts (approx. 2 to 7%). Relative contents of clay minerals generally reveal strong short-term fluctuations (Fig. 3B). However, the smoothed curves, especially of the ratios of the two dominating clay minerals smectite and illite as well as illite and chlorite (+ kaolinite), indicate precession-controlled cycles (Fig. 5). Smectite contents are higher in core intervals related to precession maxima and illite amounts increase in intervals correlated to precession minima. Only in the uppermost part of the core (approx. 10,000 to 40,000 cal. yr B.P.) it appears that these cycles do not exist. The illite/chlorite (+ kaolinite) ratio record follows the precessional cycles throughout the core with relatively higher illite abundances in intervals which correlate to minima of the precession index (Fig. 5).

Similar results are derived from crystallinity data of smectite and illite (Fig. 5): precession-controlled cycles occur in the lower part of the core with higher smectite crystallinities for the precession maxima and higher illite crystallinities for the minima. In the upper section of the core illite crystallinities remain relatively constant, while smectite crystallinities reach a distinct maximum (= minimum of the HHW, Fig. 5) near 16,000 cal. yr B.P. correlating to a maximum smectite content.

4.3. Biogenous components

The biogenic fraction of the sediment is dominated by carbonate. Carbonate contents range from approximately 8 to 22 wt% and display cyclic variations which are again precession-controlled (Fig. 4). Core intervals related to precession minima show highest $CaCO_3$ contents. Silt grain-size distributions of the carbonate fraction reveal polymodal distributions during both precession extrema. However, during precession maxima more distinct modes in the coarse silt range occur (Fig. 4). Carbonate components are dominated by nannofossils and subordinate foraminifera found in smear slide studies and shipboard results (Hebbeln et al., 1995). Siliceous microfossils only occur in minor amounts.

4.4. Spectral analyses

Spectral analyses revealed the dominance of orbital periodicities. Sub-Milankovitch frequencies only rarely reach significant spectral power (Fig. 6). The clay content, median of silt fraction, smectite/illite- and illite/chlorite + (kaolinite) ratio records have very high concentrations of spectral power in the 23 (to 19) ka precessional band (Fig. 6). Spectral peaks at 23 ka reach up to 55% of the total variance while those at the remaining orbital periodicities at 100 ka and 41 ka reveal comparatively low variance. Though the records of illite crystallinity and $CaCO_3$ content are also dominated by precessional frequencies, a significantly higher variance occurs at 41 ka within the obliquity band (Fig. 6). The $\delta^{18}O$ record reveals a strong 41 ka obliquity spectral peak. The spectral power of precessional periodicities remains below the significance level in this record (Fig. 6). Cross-spectral analyses indicate that grain-size and clay mineralogical data do not reveal significant phase differences neither among each other nor to the precession index.

5. Discussion

5.1. Sedimentological data

Cyclic variations of bulk- and silt grain-size parameters in tune with Earth's orbital precession may be explained by (a) variations of provenance due to spatial changes of the catchment area, (b) modifications of the weathering regime, and (c) a variable mode of terrigenous sediment input in response to climatic changes. Additionally, (d) variations of marine (re)sedimentation processes have to be considered.

(a) Spatial modifications of continental catchment areas can contribute to the precessional grain-size variations through controlling the relative contribution of Andean and Coastal Range source rocks. The Coastal Range is dominated by plutonic rocks, revealing a coarser-grained primary texture, compared to volcanic rocks, as primarily found in the Andes, especially north of 27.5°S where Quaternary volcanism occurs (Fig. 1B). Therefore, finer-grained sediments in core intervals correlated to precession

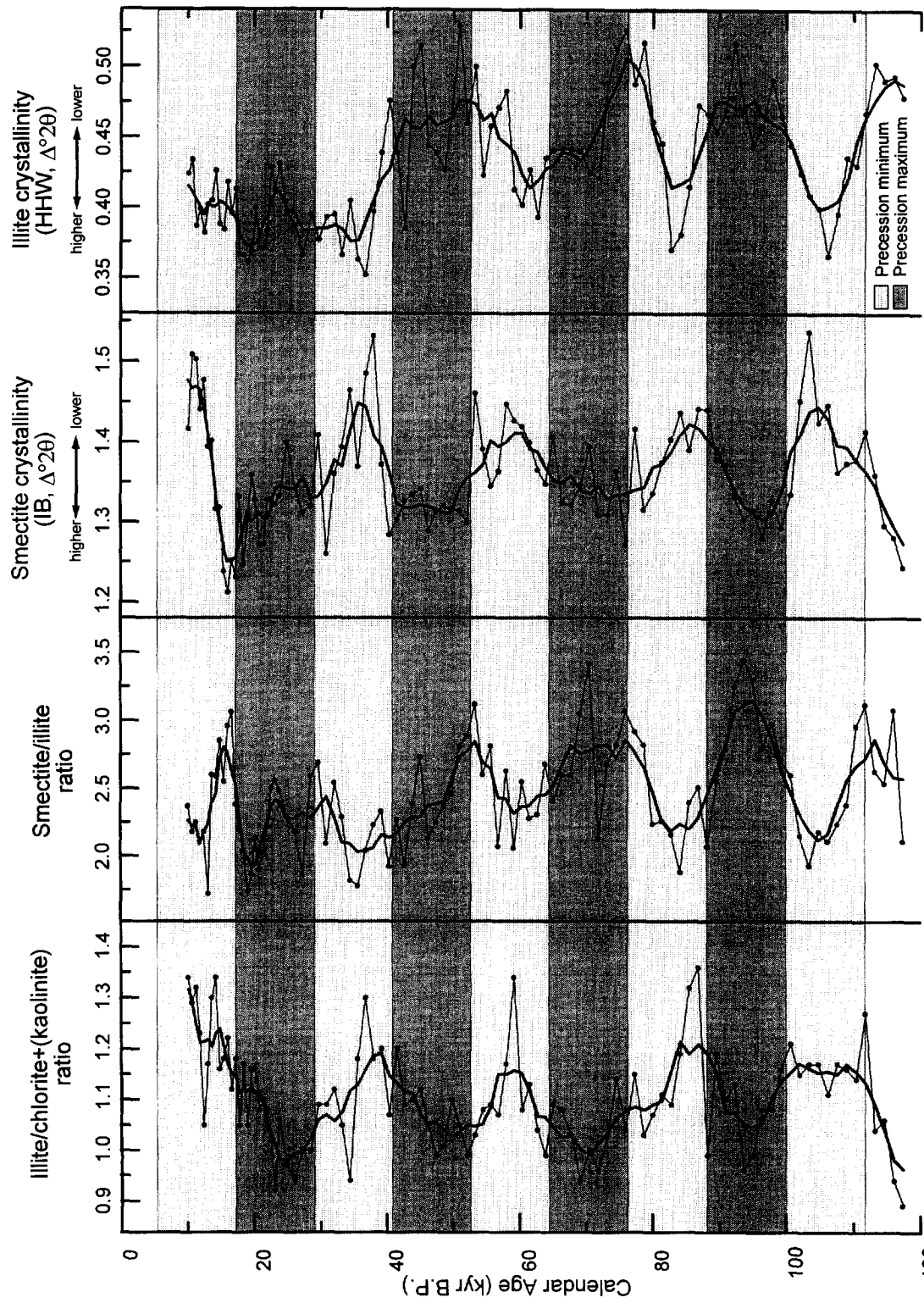

Fig. 5. Clay mineralogical data: ratios of relative contents of illite to chlorite (+ kaolinite) and smectite to illite. Smectite crystallinity is computed as IB and illite crystallinity computed as HHW (smaller values correspond to higher crystallinity). Original data are indicated by small circles and plotted as thin lines; thick lines are smoothed (as in Fig. 4). Core intervals related to precession minima are marked in light grey and those relating to precessional maxima in dark grey.

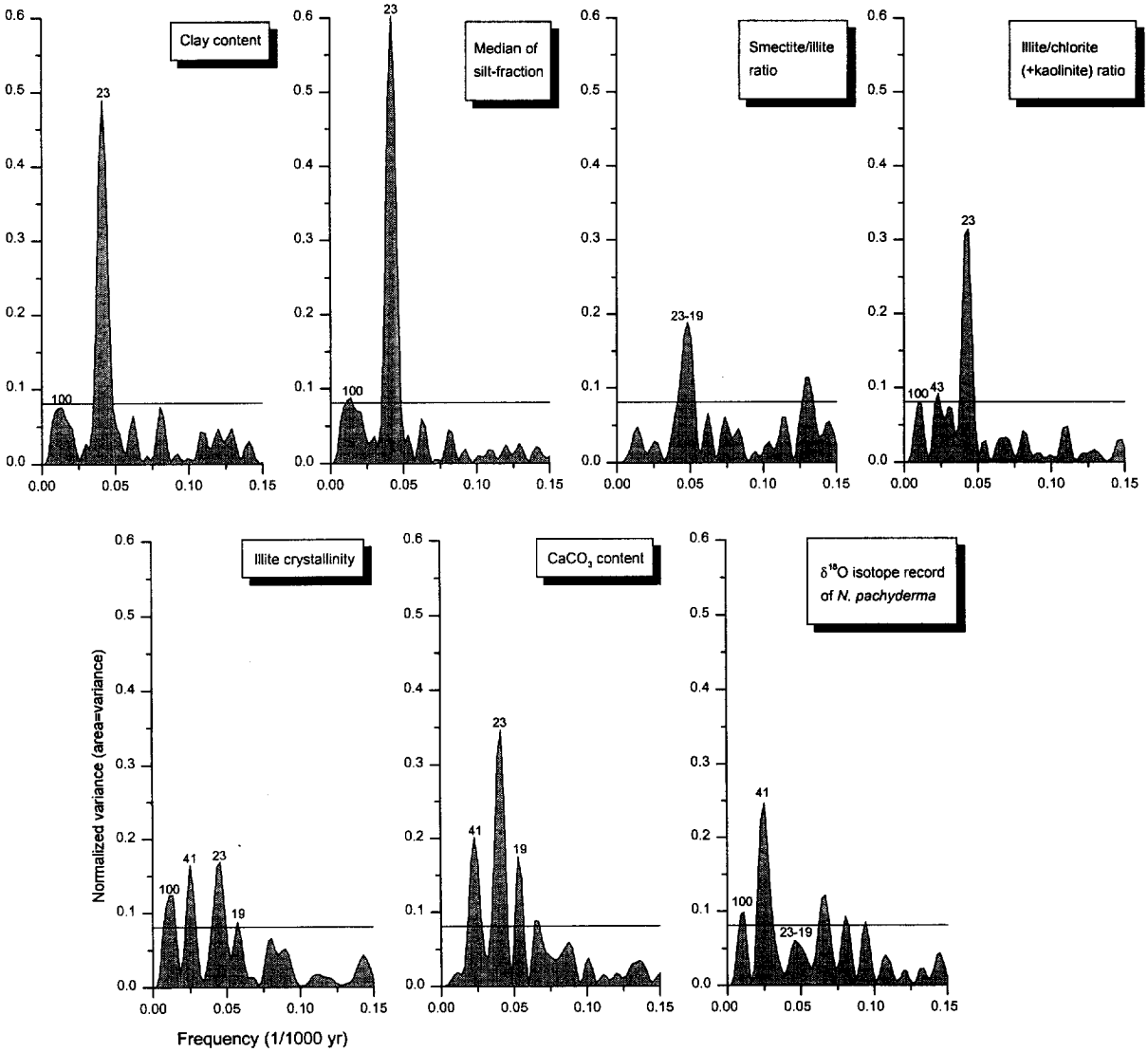

Fig. 6. Power spectra of principal grain-size, clay mineralogical, carbonate content, and $\delta^{18}O$ records. Spectra were calculated from harmonic analyses of each parameter after Schulz (1994) without time-interpolation. (6 dB bandwidth = 0.0112 ka^{-1}; significance level $\alpha = 0.05$; linear trend subtracted.) Horizontal lines indicate critical level for Siegel test (Siegel, 1980). Spectral peaks of Milankovitch frequencies are labeled.

maxima indicate higher source rock influence of the northern Andean segment and thus wider catchment areas. The coarser sediment texture for precessional minima points to source areas predominantly located in the Coastal Range, implying limited catchment areas.

(b) Chemical weathering leads to more complete grain-size reduction of the source material. Thus, generally coarser grained sediment in core intervals correlated to precession minima (Fig. 3) indicates prevailing physical weathering, whereas finer bulk and silt grain-sizes, coinciding with precessional maxima, imply increased chemical weathering rates.

(c) Silt grain-size parameters, especially the contrasting silt grain-size distributions for precessional extrema (Fig. 4), indicate that significant variations

of the mode of sediment input occurred. The shape of the grain-size distribution curves in core intervals related to precession minima, and the respective statistical parameters median and sorting (Fig. 4), point to notable aeolian sediment supply. They show marked similarities to grain-size distributions which are found in shelf and slope sediments off northern Africa (e.g. Koopmann, 1981; Sarnthein et al., 1984) as well as in abyssal sediments of the Pacific Ocean area (Rea and Hovan, 1995), both dominated by aeolian sediment input. However, rapid episodic sediment input in connection with continental flash-floods might result in similar silt grain-size distributions. Due to the extremely narrow shelf, very small amounts of sediment are trapped nearshore. On the other hand, fluviatile sediment input produces grain-size distributions (e.g. Sarnthein et al., 1984; Rea and Hovan, 1995) which resemble our data for precession maxima.

(d) Resedimentation processes, in this case variable turbidity- and bottom current activity, probably did not alter the grain-size signal, even though the detection of very fine grained turbidites and contourites and their differentiation is very difficult (e.g. Faugères and Stow, 1993). However, visual examination of the sediment core did not reveal any hints for turbidites and/or contourites throughout the core. Pathways of turbidity currents are channelized and restricted to rare submarine canyons on the continental slope off Northern Chile (Thornburg and Kulm, 1987a). Bottom-current-induced influences on the grain-size data can be excluded by comparing silt grain-size distributions of the carbonate-free sediment and the carbonate fraction (Fig. 4). Assuming that significant bottom current activity occurred, the silt grain-size distributions of the carbonate-free, terrigenous fraction and the carbonate fraction should reveal similar patterns (Wang and McCave, 1990). Our data indicate the opposite effect: in core intervals related to precession maxima (finer grained carbonate-free silt fraction) the carbonate fraction contains even higher amounts of coarse silt.

In summary, each of the factors discussed above, (a) to (c), can explain the cyclic variations of grain-size properties, but most probable is a combination of all three leading to predominating plutonic source rock contribution of the Coastal Range, implying limited catchment areas, prevailing physical weathering, and aeolian sediment input for precessional minima. During times coinciding with precession maxima the greater part of the terrigenous material probably originates from the northern Andean segment (north of 27.5°S, Fig. 1B), implying significantly wider catchment areas, and increased chemical weathering intensity providing finer-grained source material to be transported by rivers to the ocean.

Similar palaeoenvironmental reconstructions are derived from our clay mineralogical data. Generally higher illite contents correlate to better illite crystallinities during precession minima (Fig. 5). Higher illite contents may be caused by the source rock distribution as illite preferentially forms from plutonic source rocks (Chamley, 1989). This again indicates predominating source rock contribution of the Coastal Range and the southern Andean segment (south of 27.5°S) at precession minima. Additionally, high illite contents point to increased physical weathering activity (Singer, 1984; Chamley, 1989). These findings are consistent with the above interpretations (a) and (b). Further evidence for the weathering regime can be derived from the illite crystallinity, which is thought to reflect the chemical weathering intensity of the source area (Singer, 1984; Chamley, 1989). Stronger chemical weathering leads to an 'opening' of the illite structure (i.e. poor crystallinity). Thus, well crystallized illite indicates less hydrolyzing power capacity of the source environment due to more arid climatic conditions and/or lower temperature (see below).

Smectite is generally better crystallized and contents are higher during precessional maxima (Fig. 5), implying a source rock signal and possibly also increased smectite neoformation. In terms of a source rock signal higher smectite contents point to a greater contribution from volcanic rocks (Chamley, 1989) and therefore again to increased sediment input originating from the northern Andean segment. As modern continental smectite formation is favoured by semiarid climates with seasonal precipitation (Singer, 1984; Chamley, 1989), this mineral can therefore be directly interpreted palaeoclimatically.

Well formed cycles of the illite/chlorite (+ kaolinite) ratio record principally imply a source rock signal because both minerals preferentially form under prevailing physical weathering. While illite reflects

primarily the abundance of plutonic source rocks in the Coastal Range (see above), chlorite develops from low-grade metamorphic and altered basic igneous rocks (Chamley, 1989; Weaver, 1989; Hillier, 1995). Metamorphic rocks occur in the Coastal Range as well as in the Andes south of 27.5°S (Fig. 1B). Tertiary to Recent volcanics of the Andes are predominately intermediate. More basic igneous rocks include mainly marine volcanics on the Andean side of the Coastal Range (Fig. 1B). Therefore the source areas of chlorite are not easy to define but, in combination with the above findings, an increased fluvial input of chlorite from more inland areas is likely for times of precessional maxima.

The reconstructions of the terrestrial sedimentary environment derived from our sedimentological data can be best explained palaeoclimatically in terms of a precipitation signal (Fig. 7). For times coinciding with precession minima limited catchment areas, prevailing physical weathering, and increased aeolian sediment input imply enhanced aridity, possibly episodically interrupted by catastrophic precipitation events leading to flash-floods. In contrast to this, for the precession maxima more humid conditions with seasonal precipitation are concluded from wider catchment areas, stronger chemical weathering, continental smectite neoformation, and predominating fluvial sediment input.

In the records of smectite, as well as illite content and crystallinity, precessional cycles seem to be less evolved or absent in the uppermost part of the core (Fig. 5), in contrast to the illite/chlorite (+ kaolinite) ratio and grain-size data. Smectite in particular might also originate from lateral transport by oceanic currents due to its extremely small grain size, even for clay minerals. Additionally, authigenic sources (i.e. alteration of volcanic glass) of smectite have to be considered, especially for the distinct smectite content maximum correlating to a high smectite crystallinity (Fig. 5). However, smear slide analyses showed only minor amounts of volcanic glass throughout the core, which was mainly unaltered. The rather constant high illite crystallinities (= low values of HHW, Fig. 5) approximately correspond

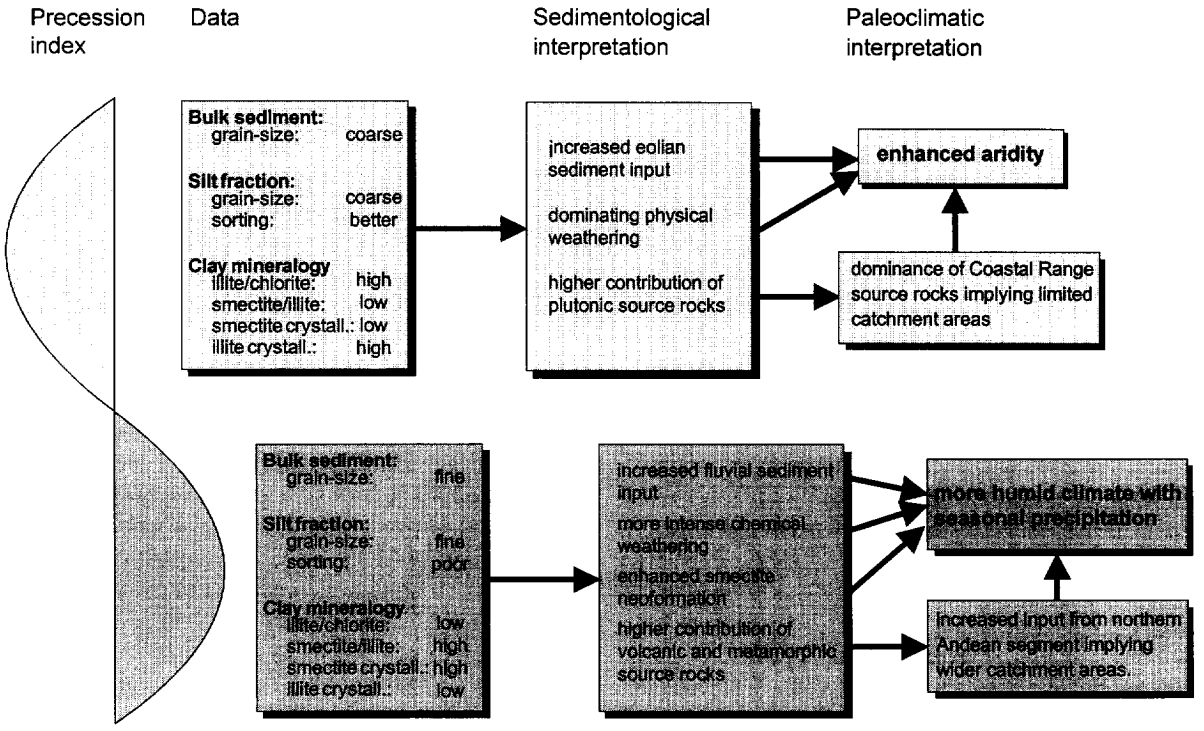

Fig. 7. Summary of contrasting data and resulting sedimentological, as well as palaeoclimatic interpretations for times related to precession minima (light grey) and precession maxima (dark grey).

to the coldest parts of the last glacial. This might indicate that the continental chemical weathering intensity remained weak due to low temperatures even though more humid conditions prevailed during the last precession maxima.

5.2. Regional palaeoclimatic implications

The palaeoclimatic interpretations of our sedimentological data lead to the conclusion that the Late Pleistocene continental climate of Chile around latitude 27°S was characterized by alternating relatively arid and humid phases (Fig. 7). During precession minima aridity was probably even stronger than today and perennial rivers were absent. Episodic flash-floods, like those that currently occur in arid regions of northern Chile (Abele, 1989; Garleff et al., 1991), might have occurred sporadically, indicating catastrophic precipitation events. For precessional maxima we suggest a semiarid climate with seasonal precipitation similar to the mediterranean type winter-rain climate that presently occurs south of latitude 31°S (Fig. 1A). Precipitation was sufficient to evolve a perennial river system probably including the recent dry valleys (Fig. 1B) and led to significant additional sediment input originating from the northern segment of the Andes (north of 27.5°S).

Regional palaeoclimatic reconstructions focus primarily on the Last Glacial Maximum (LGM) and the Holocene. The LGM is equivalent to the precession maximum centred around 22,000 cal. yr B.P. (Fig. 2). Thus our palaeoclimatic record indicates relatively humid conditions for the LGM. Our data set does not cover the Holocene.

There are two opposing views about the palaeoclimate of Chile during the LGM, based primarily on palynological data of mid-latitude Chile and Argentina between 34°S and 45°S. One postulates a latitudinal equatorward shift by at least 5° of the westerly precipitation belt resulting in a more humid climate for central Chile during the LGM (Heusser, 1989, 1990). The second proceeds on the assumption that generally arid and cold conditions prevailed except for a narrow band at latitudes from 43° to 45°S. The latter originates from a poleward shift, a latitudinal compression and intensification of the westerly storm tracks (Markgraf et al., 1992). Modelling of annual rainfall and snowline levels in central Chile between 30° and 43°S (Caviedes, 1990) as well as Patagonia (40°S to 56°S; Hulton et al., 1994) support Heusser's view of a northward shift of the Southern Westerlies.

For the closer surroundings of our study area an increased influence of the Southern Westerlies during the LGM is generally rejected. Veit (1992, 1996) found geomorphic and pedologic evidence for increased westerly precipitation at latitudes from 27° to 33°S only for the Holocene and Fox and Strecker (1991) concluded that moist westerlies did not significantly affect the Andes north of 28°S during the Late Pleistocene. However, a more humid mediterranean-type climate in our investigation area around 27°S during the LGM conforms to a northward shift of the climatic zones of Chile (Fig. 1A) and thus probably also to an equatorward movement of the Southern Westerlies. A subtropical Atlantic–Amazonian source of moisture, as proposed for late-glacial humid phases on the Altiplano at 21° to 24°S (Grosjean, 1994, Grosjean et al., 1995), but also for mid-latitude Chile (Markgraf, 1989) is improbable for our study area for two reasons. Firstly, the late-glacial humid Tauca phase on the Altiplano occurred significantly later (approx. 10,000 to 15,000 ^{14}C yr B.P., e.g. Servant et al., 1995; Clapperton et al., 1997) than the humid time span around the LGM in our record. Secondly, an influx of subtropical moisture from the northeast would mean a crossing of the South American arid diagonal zone which is thought to have remained in a stable position throughout the Late Quaternary (Garleff et al., 1991).

Pre-LGM palaeoclimatic records are sparse in southern South America. However, arid–humid climatic cycles over the last >50,000 ^{14}C yr B.P., as reconstructed from the palynological record of Laguna de Tagua Tagua (mid-latitude Chile, 34°S; Heusser, 1984, 1990), are identical with those deduced from our data (Fig. 8). The palynological record is also interpreted to reflect precipitation changes due to latitudinal shifts of the Southern Westerlies. This further emphasizes an identical moisture source for pre-LGM precipitation variations in our record. The palaeoclimatic interpretation of glacier fluctuations in southernmost Chile (Southern Patagonia; Clapperton et al., 1995), covering the last glacial cycle, also supports our results. In this study reduced ice extent during the LGM and earlier parts of the last glacial has been interpreted in terms of less precipitation due

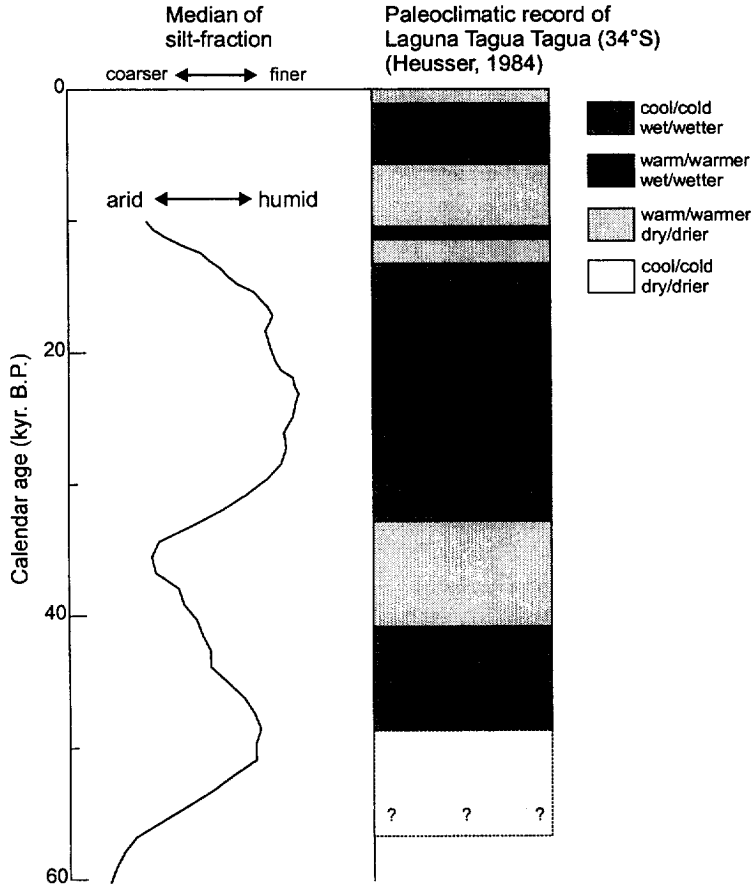

Fig. 8. Comparison of palaeoclimatic record of Laguna de Tagua Tagua (after Heusser, 1984; based on palynological data) and climatic cycles deduced from sedimentological data in this study, as represented by the smoothed median record (see Fig. 4 for scale).

to an equatorward shift of the Southern Westerlies consistent with our data.

Indications of episodic flash-floods during precession minima might be explained by more abundant El Niño events resulting in torrential storms. Correspondingly, El Niño events were possibly less frequent or absent during precessional maxima which approximately correspond to global glacial maxima (i.e. marine isotope stages 2 and 4). This is in agreement with the assumption that the El Niño Southern Oscillation was reduced or totally absent during glacial maxima (e.g. Mörner, 1993; Ortlieb and Macharé, 1993).

5.3. Global palaeoclimatic implications

The majority of the analysed sedimentological parameters in the investigated sediment core is strongly dominated by a precession-controlled cyclicity (Fig. 6) which we primarily interpret in terms of changes in precipitation. Precessional forcing of low-latitude palaeoclimatic records has been identified extensively in the Northern Hemisphere, especially in tropical Africa and the adjacent eastern Atlantic (review in deMenocal et al., 1993). The inferred continental palaeoclimatic cycles reveal principally precipitation changes (deMenocal et al., 1993) and are mainly controlled by a linear response of the monsoonal circulation system to low-latitude insolation variations (e.g. Rossignol-Strick, 1983; Prell and Kutzbach, 1987, 1992; McIntyre et al., 1989). For the Northern Hemisphere monsoon higher rainfall generally occurs during precession minima which are equivalent to boreal summer insolation maxima. Correspondingly, in the Southern Hemisphere stronger

monsoonal rainfall should be expected during precessional maxima, as in our records, coinciding with austral summer insolation maxima. However, for reasons discussed above, the South American monsoonal circulation system does not affect our study area. Even northeast of the South American arid diagonal zone low-latitude insolation forcing is not straightforward: the late-glacial to early Holocene humid Tauca phase coincides to a precession minimum (Grosjean et al., 1995), whereas further northeast several palaeoenvironmental records indicate more arid conditions, as expected from austral summer insolation induced monsoonal forcing (Martin et al., 1997).

As discussed previously, we suggest that precipitation changes in our study area are most likely due to latitudinal shifts of the Southern Westerlies. Thus, the latitudinal position of this extratropical circulation system varies with the precessional orbital cycle. Latitudinal movements of the Southern Westerlies have also been deduced from marine geological data of the South Atlantic (Jansen et al., 1996) and southern Indian Ocean (Morley, 1989; Howard and Prell, 1992). Jansen et al. (1996) proposed that the shifts of the westerly belt are probably induced by precessional growth and decay of the sea ice fields in the Southern Ocean.

Meteorological studies indicate that enhanced east–west circulation in the tropical South Atlantic leads to a weakening of the Hadley-type circulation in the South American–Southeast Pacific sector (Pittock, 1980). The strength of the South Atlantic zonal circulation, as reflected by the zonality of the trade winds, varied in phase with boreal summer insolation, indicating stronger zonal trade winds during precession maxima (e.g. Schneider et al., 1995). This would imply a weakened Hadley cell over the Southeast Pacific during precession maxima which should facilitate an equatorward movement of the Southern Westerlies as attested by our data. The precession controlled latitudinal movements may therefore depend on interoceanic teleconnections forced by low-latitude Northern Hemisphere insolation.

The illite crystallinity, $CaCO_3$ content and $\delta^{18}O$ records reveal significantly higher spectral power in the obliquity (41 ka) band (Fig. 6). For the illite crystallinity, as discussed above, this can be interpreted in terms of a continental temperature signal, which likely reflects a stronger influence of high-latitude forcing. The carbonate signal is probably primarily forced by marine biological productivity changes due to variations of the upwelling intensity. The latter is also dominated by precessional cycles off northern Chile (J. Klump, pers. commun., 1997). However, variations of the Chile Coastal- and Humboldt Currents might introduce a higher latitude temperature signal in response to obliquity. The spectral data of the $\delta^{18}O$ signal reflect primarily the global ice volume and thus high latitude control (e.g. Imbrie et al., 1992, 1993).

The absence of significant phase differences among our terrigenous sedimentological proxies and the precession index points to a very rapid response of the continental sedimentary system to climatic and hydrologic changes which themselves react immediately to precessional insolation changes. Previously observed phase lags between proxies of the continental palaeoclimate of Africa and the precessional cycle have been proved to be an artifact of the ^{14}C chronology and nearly disappear if ^{14}C-ages are converted to calendar years (deMenocal et al., 1993).

6. Conclusions

Cyclic variations of grain-size and clay mineralogical parameters of Late Quaternary terrigenous sediments from the Chilean continental slope (27°S) can be interpreted in terms of significant changes of sediment provenance, weathering regimes in the source areas, and modes of sediment input from the adjacent continent. The interpretation of these findings provides an extended palaeoclimate model for northern Chile, which for the first time comprises the last 120,000 years.

Our data indicate alternating arid phases, when aridity was probably even more severe than today, in contrast to relatively humid time spans with seasonal rainfall and a precipitation regime similar to that of the modern mediterranean type climate of central Chile.

Spectral analyses reveal that the cycles of the terrigenous sedimentological proxies are strongly controlled by Earth's orbital precession. The absence of significant phase differences among the proxies and between the proxies and the precession index demonstrates the rapid response of the continental sedimentary environment to insolation changes.

Variations of palaeotemperature in the 41 ka obliquity band, as indicated by down-core fluctuations of illite crystallinity, document that shorter-term precessional cycles of palaeohumidity were overprinted by long-term temperature changes in tune with high-latitude forcing.

Increased aridity during precession minima in contrast to humid conditions during precession maxima (including the LGM) point to latitudinal shifts of the Southern Westerlies. Precessional forcing of latitudinal movements of the westerly atmospheric circulation system may be conceivable through teleconnections to the Northern Hemisphere monsoonal system in the Atlantic Ocean region.

Acknowledgements

We thank the captain and crew of RV *Sonne* for their excellent help with coring and sampling operations during cruises in the Southeast Pacific. Analytical assistance was provided by B. Diekmann, G. Kuhn, R. Fröhlking, S. Janisch and H. Rhodes at the Alfred Wegener Institute in Bremerhaven. B. Diekmann also gave many helpful comments to an earlier version of the manuscript. We also thank M. Segl and B. Meyer-Schack for oxygen isotope measurements. Financial support was provided by the German Bundesministerium für Bildung und Forschung through funding the project *CHIPAL* (03G0102A).

References

Abele, G., 1989. Hygrisches Klima und Talbildung auf der Westflanke der zentralen Anden. Geoökodynamik 10, 253–276.

Bard, E., 1988. Correction of accelerator mass spectrometry ^{14}C ages measured in planktonic foraminifera: paleoceanographic implications. Paleoceanography 3, 635–645.

Bard, E., Arnold, M., Fairbanks, R.G., Hamelin, B., 1993. ^{230}Th–^{234}U and ^{14}C ages obtained by mass spectrometry of corals. Radiocarbon 35 (1), 191–199.

Berger, A., Loutre, M.F., 1991. Insolation values for the climate of the last 10 million years. Quat. Sci. Rev. 10, 297–317.

Biscaye, P.E., 1965. Mineralogy and sedimentation of recent deep-sea clay in the Atlantic Ocean and adjacent seas and oceans. Geol. Soc. Am. Bull. 76, 803–832.

Blackman, R.B., Tukey, J.W., 1958. The Measurement of Power Spectra. Dover Publications, New York, 190 pp.

Caviedes, C., 1990. Rainfall variation, snowline depression and vegetational shifts in Chile during the Pleistocene. Climatic Change 16, 94–114.

Chamley, H., 1989. Clay Sedimentology. Springer, Berlin, 623 pp.

Clapperton, C.M., 1993. Nature of environmental changes in South America at the Last Glacial Maximum. Palaeogeogr., Palaeoclimatol., Palaeoecol. 101, 189–208.

Clapperton, C.M., Sugden, D.E., Kaufman, D.S., McCulloch, R.D., 1995. The last glaciation in Central Magellan Strait, southernmost Chile. Quat. Res. 44, 133–148.

Clapperton, C.M., Clayton, J.D., Benn, D.I., Marden, C.J., Argollo, J., 1997. Late Quaternary glacier advances and palaeolake highstands in the Bolivian Altiplano. Quat. Int. 38, 49–59.

deMenocal, P.B., Ruddiman, W.F., Pokras, E.M., 1993. Influences of high- and low-latitude processes on African terrestrial climate: Pleistocene eolian records from equatorial Atlantic Ocean Drilling Program Site 663. Paleoceanography 8 (2), 209–242.

Faugères, J.C., Stow, D.A.V., 1993. Bottom-current controlled sedimentation: a synthesis of the contourite problem. Sediment. Geol. 82, 287–297.

Folk, R.L., Ward, W., 1957. Brazos River bar: a study in the significance of grain size parameters. J. Sediment. Petrol. 27, 3–26.

Fox, A.N., Strecker, M.R., 1991. Pleistocene and modern snowlines in the Central Andes (24–28°S). Bamberger Geogr. Schr. 11, 169–182.

Garleff, K., Schäbitz, F., Stingl, H., Veit, H., 1991. Jungquartäre Landschaftsentwicklung beiderseits der Ariden Diagonale Südamerikas. Bamberger Geogr. Schr. 11, 359–394.

Grosjean, M., 1994. Paleohydrology of the Laguna Lejia (north Chilean Altiplano) and climatic implications for late-glacial times. Palaeogeogr., Palaeoclimatol., Palaeoecol. 109, 89–100.

Grosjean, M., Messerli, B., Ammann, C., Geyh, M.A., Graf, K., Jenny, B., Kammer, K., Nuñez, L., Schreier, H., Schotterer, U., Schwalb, A., Valero-Garcés, B.V., Vuille, M., 1995. Holocene environmental changes in the Atacama Altiplano and paleoclimatic implications. Bull. Inst. Fr. Étud. Andines 24 (3), 585–594.

Hebbeln, D., Wefer, G., et al., 1995. Cruise Report of R/V SONNE Cruise 102, Valparaiso–Valparaiso, 9.5.–28.6.95. Berichte Fachbereich Geowissenschaften, Universität Bremen, 68, 126 pp.

Heusser, C.J., 1984. Late Quaternary climates of Chile. In: Vogel, J.C. (Ed.), Late Cenozoic Palaeoclimates of the Southern Hemisphere. Balkema, Rotterdam, pp. 59–83.

Heusser, C.J., 1989. Southern westerlies during the Last Glacial Maximum. Quat. Res. 31, 423–425.

Heusser, C.J., 1990. Ice age vegetation and climate of subtropical Chile. Palaeogeogr., Palaeoclimatol., Palaeoecol. 80, 107–127.

Hillier, S., 1995. Erosion, sedimentation and sedimentary origin of clays. In: Velde, B. (Ed.), Origin and Mineralogy of Clays. Springer, Berlin, 334 pp.

Howard, W.R., Prell, W.L., 1992. Late Quaternary surface circulation of the southern Indian Ocean and its relationship to orbital variations. Paleoceanography 7 (1), 79–117.

Hulton, N., Sugden, D., Payne, A., Clapperton, C., 1994. Glacier modeling and the climate of Patagonia during the Last Glacial Maximum. Quat. Res. 42, 1–19.

Imbrie, J., Hays, J.D., Martinson, D.G., McIntyre, A., Mix, A.C., Morley, J.J., Pisias, N.G., Prell, W.L., Shackleton, N.J., 1984. The orbital theory of Pleistocene climate: support from a revised chronology of the marine $\delta^{18}O$ record. In: Berger, A.L., Imbrie, J., Hays, J.D., Kukla, G., Saltzmann, B. (Eds.), Milankovitch and Climate, Part I. Reidel, Norwell, Mass., pp. 269–305.

Imbrie, J., Boyle, E.A., Clemens, S.C., Duffy, A., Howard, W.R., Kukla, G., Kutzbach, J., Martinson, D.G., McIntyre, A., Mix, A.C., Molfino, B., Morley, J.J., Peterson, L.C., Pisias, N.G., Prell, W.L., Raymo, M.E., Shackleton, N.J., Toggweiler, J.R., 1992. On the structure and origin of major glaciation cycles, 1. Linear responses to Milankovitch forcing. Paleoceanography 7 (6), 701–738.

Imbrie, J., Berger, A., Boyle, E.A., Clemens, S.C., Duffy, A., Howard, W.R., Kukla, G., Kutzbach, J., Martinson, D.G., McIntyre, A., Mix, A.C., Molfino, B., Morley, J.J., Peterson, L.C., Pisias, N.G., Prell, W.L., Raymo, M.E., Shackleton, N.J., Toggweiler, J.R., 1993. On the structure and origin of major glaciation cycles, 2. The 100,000 year cycle. Paleoceanography 8 (6), 699–735.

Ingle, J.C., Keller, G., Kolpack, R.L., 1980. Benthic foraminiferal biofacies, sediments and water masses of the southern Peru–Chile Trench area, southeastern Pacific Ocean. Micropaleontology 26, 113–150.

Jansen, J.H.F., Ufkes, E., Schneider, R.R., 1996. Late Quaternary movements of the Angola–Benguela Front, SE Atlantic, and implications for advection in the equatorial ocean. In: Wefer, G., Berger, W.H., Siedler, G., Webb, D.J. (Eds.), The South Atlantic: Present and Past Circulation. Springer, Berlin, pp. 553–575.

Johnson, D.R., Fonseca, T., Sievers, H., 1980. Upwelling in the Humboldt Coastal Current near Valparaiso, Chile. J. Mar. Res. 38 (1), 1–15.

Jones, K.P.N., McCave, I.N., Patel, P.D., 1988. A computer-interfaced sedigraph for modal size analysis of fine-grained sediment. Sedimentology 35, 163–172.

Jordan, T.E., Isacks, B.L., Allmendinger, R.W., Brewer, J.A., Ramos, V.A., Ando, C.J., 1983. Andean tectonics related to geometry of subducted Nazca plate. Geol. Soc. Am. Bull. 94, 341–361.

Koopmann, B., 1981. Sedimentation von Saharastaub im subtropischen Nordatlantik während der letzten 25000 Jahre. Meteor Forschungsergeb., Reihe C 35, 23–59.

Lamy, F., Hebbeln, D., Wefer, G., submitted. Terrigenous sediment supply along the Chilean continental slope: modern regional patterns of texture and composition. Geol. Rundsch.

Lowell, T.V., Heusser, C.J., ersen, B.G., Moreno, P.I., Hauser, A., Heusser, L.E., Schlüchter, C., Marchant, D.R., Denton, G.H., 1995. Interhemispheric correlation of Late Pleistocene glacial events. Science 269, 1541–1549.

Markgraf, V., 1989. Reply to C.J. Heusser's 'Southern Westerlies' during the Last Glacial Maximum. Quat. Res. 31, 426–432.

Markgraf, V., Dodson, J.R., Kershaw, P.A., McGlone, M.S., Nicholls, N., 1992. Evolution of late Pleistocene and Holocene climates in the circum-South Pacific land areas. Clim. Dyn. 6, 193–211.

Martin, L., Bertoux, J., Gorrege, T., Ledru, M.P., Mourguiart, P., Sifeddine, A., Soubies, F., Wirrmann, D., Suguio, K., Turcq, B., 1997. Astronomical forcing of contrasting rainfall changes in tropical South America between 12,400 and 8,800 cal yr B.P. Quat. Res. 47, 117–122.

McCave, I.N., Manighetti, B., Robinson, S.G., 1995. Sortable silt and fine sediment size/composition slicing: parameters for palaeocurrent speed and palaeoceanography. Paleoceanography 10 (3), 593–610.

McIntyre, A., Ruddiman, W.F., Karlin, K., Mix, A.C., 1989. Surface water response of the equatorial Atlantic Ocean to orbital forcing. Paleoceanography 4, 19–55.

Miller, A., 1976. The climate of Chile. In: Schwerdtfeger (Ed.), World Survey of Climatology Vol. 12. Elsevier, Amsterdam, pp. 113–145.

Milliman, J.D., Rutkowski, C., Meybeck, M., 1995. River discharge to the sea: a global river index (GLORI). LOICZ reports and studies, NIOZ, Texel, 125 pp.

Morley, J.J., 1989. Variations in high-latitude oceanographic fronts in the southern Indian Ocean: an estimation based on faunal changes. Paleoceanography 4 (5), 547–554.

Mörner, N.A., 1993. Present El Niño–ENSO events and past super-ENSO events. Bull. Inst. Fr. Étud. Andines 22 (1), 3–12.

Müller, G., 1967. Methods in Sedimentary Petrology. Schweizerbart'sche, Stuttgart, 283 pp.

Nadeau, M.J., Schleicher, M., Grootes, P.M., Erlenkeuser, H., Gottolang, A., Mous, D.J.W., Sarnthein, J.M., Willkomm, H., 1997. The Leibniz-Labor AMS facility at the Christian-Albrechts University, Kiel, Germany. Nucl. Instrum. Methods Phys. Res. 123, 22–30.

Ortlieb, L., Macharé, J., 1993. Former El Niño events: records from western South America. Global Planet. Change 7, 181–202.

Petschick, R., Kuhn, G., Gingele, F., 1996. Clay mineral distribution in surface sediments of the South Atlantic: sources, transport and relation to oceanography. Mar. Geol. 130, 203–229.

Pittock, A.B., 1980. Patterns of climatic variation in Argentina and Chile-I. Precipitation, 1931–60. Mon. Weather Rev. 108, 1347–1361.

Prell, W.L., Kutzbach, J.E., 1987. Monsoon variability over the past 150,000 years. J. Geophys. Res. 92, 8411–8425.

Prell, W.L., Kutzbach, J.E., 1992. Sensitivity of the Indian monsoon to forcing parameters and implications for its evolution. Nature 360, 647–652.

Rea, D.K., Hovan, A., 1995. Grain-size distribution and depositional processes of the mineral component of abyssal sediments: lessons from the North Pacific. Paleoceanography 10 (2), 251–258.

Rossignol-Strick, M., 1983. African monsoons, an immediate climatic response to orbital insolation. Nature 303, 46–49.

Sarnthein, M., Thiede, J., Pflaumann, H., Erlenkeuser, H., Fütterer, D., Koopmann, B., Lange, H., Seibold, E., 1984. Atmo-

spheric and oceanic circulation patterns off Northwest Africa during the past 25 million years. In: von Rad, H., Hinz, K., Sarnthein, M., Seibold, E. (Eds.), Geology of the Northwest African Continental Margin. Springer, Berlin, pp. 584–604.

Schneider, R., Müller, P.J., Ruhland, G., 1995. Late Quaternary surface circulation in the east equatorial South Atlantic: evidence from alkenone sea surface temperatures. Paleoceanography 10 (2), 197–219.

Scholl, D.W., Christensen, M.N., Von Huene, R., Marlow, M.S., 1970. Peru–Chile Trench sediments and sea-floor spreading. Geol. Soc. Am. Bull. 81, 1339–1360.

Schulz, M., 1994. Spektralanlyse nicht äquidistanter paläoklimatischer Zeitreihen: SPECTRUM — ein Turbo Pascal Programm. Diplomarbeit, Univ. of Kiel, 142 pp.

Servant, M., Fournier, M., Argollo, J., Servant-Vildary, S., Sylvestre, F., Wirrmann, D., Ybert, J.P., 1995. La dernière transition glaciaire/interglaciaire des Andes tropical sud (Bolivie) d'après l'étude des variations des niveaux lacustres et des fluctuations glaciaires. C. R. Acad. Sci. Paris, Sér. II 320, 729–736.

Shaffer, G., Salinas, S., Pizarro, O., Vega, A., Hormazabal, S., 1995. Currents in the deep ocean off Chile (30°S). Deep Sea Res. 42, 425–436.

Siegel, A.F., 1980. Testing the periodicity in a time series. J. Am. Statist. Assoc. 75, 345–348.

Singer, A., 1984. The paleoclimatic interpretation of clay minerals in sediments — a review. Earth Sci. Rev. 21, 251–293.

Stein, R., 1985. Rapid grain-size analyses of clay and silt fraction by Sedigraph 5000D: comparison with Coulter Counter and Atterberg methods. J. Sediment. Petrol. 55 (4), 590–615.

Strub, P.T., Mesias, J.M., Montecino, V., Ruttlant, J., Salinas, S., 1998. Coastal ocean circulation off Western South America. In: The Sea (Coastal Oceans) (in press).

Syvitszki, J.P.M., 1991. Principles, Methods and Application of Particle Size Analysis. Cambridge University Press, Cambridge, 368 pp.

Thornburg, T., Kulm, L.D., 1987a. Sedimentation in the Chile Trench: depositional morphologies, lithofacies and stratigraphy. Geol. Soc. Am. Bull. 98, 33–52.

Thornburg, T., Kulm, L.D., 1987b. Sedimentation in the Chile Trench: petrofacies and provenance. J. Sediment. Petrol. 57, 55–74.

Veit, H., 1992. Jungquartäre Landschafts- und Bodenentwicklung im chilenischen Andenvorland zwischen 27–33°S. Bonner Geogr. Abh. 85, 196–208.

Veit, H., 1996. Southern Westerlies during the Holocene deduced from geomorphological and pedological studies in the Norte Chico, Northern Chile (27–33°S). Palaeogeogr., Palaeoclimatol., Palaeoecol. 123, 107–119.

Villagrán, C., 1993. Una interpretación climática del registro palinológico del último ciclo glacial–postglacial en Sudamérica. Bull. Inst. Fr. Étud. Andines 22 (1), 243–258.

Wang, H., McCave, I.N., 1990. Distinguishing climatic and current effects in mid-Pleistocene sediments of Hatton and Gardar Drifts, NE Atlantic. J. Geol. Soc. London 147, 373–383.

Weaver, C.E., 1989. Clays, Muds and Shales. Developments in Sedimentology 44, Elsevier, Amsterdam, 819 pp.

Weischet, W., 1970. Chile. Seine länderkundliche Individualität und Struktur. Wissenschafliche Buchgesellschaft, Darmstadt, 618 pp.

Zeil, W., 1986. Südamerika. Geologie der Erde Band 1, Enke, Stuttgart, 160 pp.